

Automated Discovery of Interactions and Dynamics for Large Networked Dynamical Systems

Yan Zhang¹, Yu Guo^{2,3}, Zhang Zhang¹, Mengyuan Chen¹, Shuo Wang¹, and Jiang Zhang^{1,*}

¹Beijing Normal University, Beijing, China

²State Key Laboratory for Novel Software Technology at Nanjing University, Nanjing, China

³Software Institute, Nanjing University, Nanjing, China

*zhangjiang@bnu.edu.cn

ABSTRACT

Understanding the mechanisms of complex systems is very important. Networked dynamical system, that understanding a system as a group of nodes interacting on a given network according to certain dynamic rules, is a powerful tool for modelling complex systems. However, finding such models according to the time series of behaviors is hard. Conventional methods can work well only on small networks and some types of dynamics. Based on a Bernoulli network generator and a Markov dynamics learner, this paper proposes a unified framework for Automated Interaction network and Dynamics Discovery (AIDD) on various network structures and different types of dynamics. The experiments show that AIDD can be applied on large systems with thousands of nodes. AIDD can not only infer the unknown network structure and states for hidden nodes but also can reconstruct the real gene regulatory network based on the noisy, incomplete, and being disturbed data which is closed to real situations. We further propose a new method to test data-driven models by experiments of control. We optimize a controller on the learned model, and then apply it on both the learned and the ground truth models. The results show that both of them behave similarly under the same control law, which means AIDD models have learned the real network dynamics correctly.

Introduction

Living cell, brain, human society, stock market, global climate system, and so forth are all complex systems which are composed of a large number of non-linear interactive units [1–5]. By decomposing a complex system into a static network with dynamics on nodes, networked dynamical system, as a powerful tool to describe complex systems, have played paramount roles to understand their collective behaviors and control their functions [2, 3, 6]. However, building such models requires not only professional knowledge but also experiences of modelling, this hinders wide applications of these methods. How to reconstruct such networked dynamical systems in a data-driven way, i.e., to retrieve the interaction network structure and the node dynamics from time series data of complex system behaviours without any subjective biases, is a fundamental problem [7, 8].

Although many classical approaches on time series forecasting have been proposed[9–11], how to predict the behaviors of complex systems with highly non-linear and long range correlations, especially those based on a complex network structure, has not been resolved until the recent introduction of Graph (Neural) Network (GNN) models[12–23]. GNN is designed particularly for networked dynamical systems. By learning complex functions of information aggregation and propagation on a given network, GNN can simulate any complex dynamics on this network. However, a complete graph is always required in prior for most GNN models, which hinders their wider applications[8, 21, 24–28].

A network structure, depicting how different units interact each other, is of great importance because it can help us to understand the behaviors of a complex system. The interaction network also implies a causal structure which characterises how events taking place sequentially in a causal way[5, 29–32]. Therefore revealing network structure can improve the algorithm’s explainability and transparency from the aspect of causality. The interaction or causal structure can be obtained by directly calculating some statistical measures[33–35], perturbing the system[36, 37], optimizing a score function[38, 39], or expanding the complex interaction dynamics on a set of basal functions[7, 40, 41], and other methods[42–45].

Among these algorithms, ARNI(Algorithm for revealing network interactions) is one of the most prominent model-free method. It can not only infer the network with a high accuracy, but also can adopt to various nonlinear dynamics. The fly in the ointment is that the performance of the model strongly depends on the choice of the basal functions. If the prior biases on basal functions are missing, it will be very time-consuming, which limits the applications of this approach on larger systems.

Very few studies have been proposed to do both network inference and time series forecasting tasks together although some network inference algorithms are capable of doing forecasting. The implicit and time variant network structure can also be

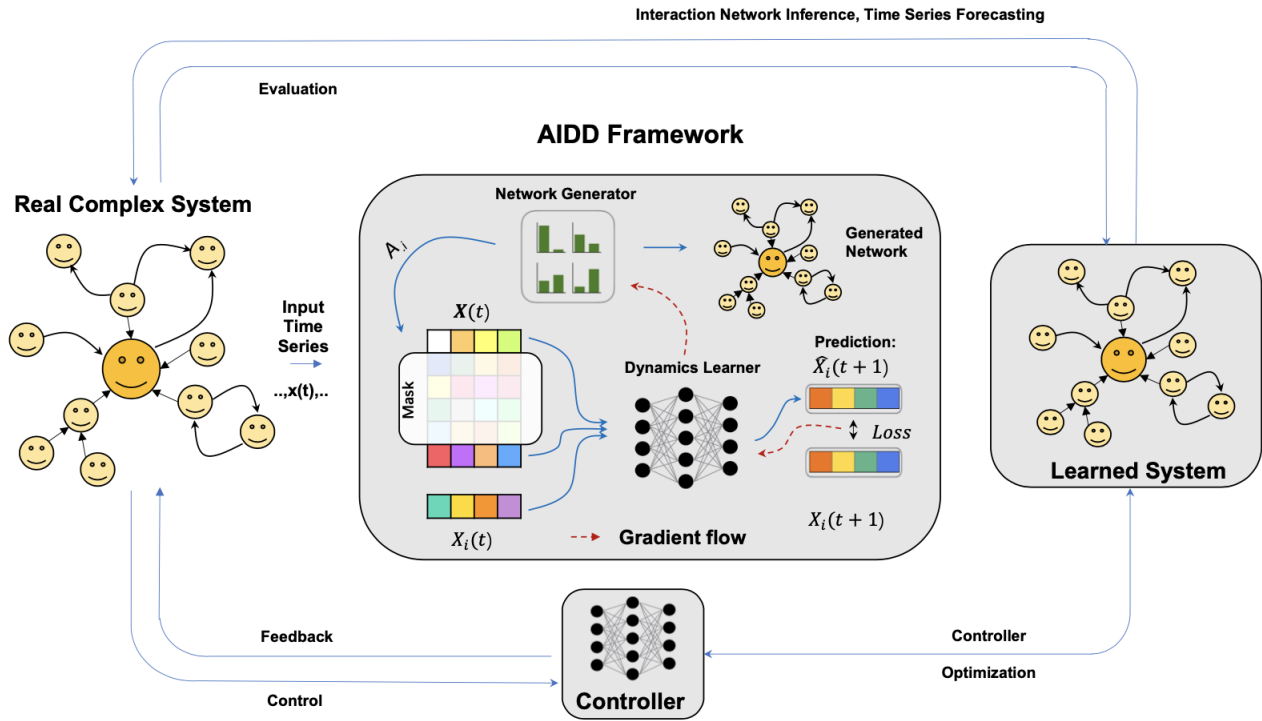


Figure 1. The workflows of how Automated Interaction and Dynamics Discovery(AIDD) framework models a complex system, and how AIDD can be evaluated by tasks of time series forecasting, interaction network inference, and control experiments. The framework of AIDD is also shown in the inset box. In which, a column of the adjacency matrix for the candidate network is sampled by the network generator. It can be regarded as a mask vector to filter out the supposed unrelated nodes. Then, the time series information for related nodes is input into a neural network, dynamics learner. It will output a prediction for the new states of all nodes. Then, the prediction is compared against the data. And the loss function can be calculated, the gradient information can be back-forward directly. After optimization, a learned networked dynamical system represented by neural networks can be obtained.

obtained from the deep learning models for forecasting based on attention mechanism[8, 27, 46–50]. The first framework to derive an explicit network is the model of Neural Relation Inference (NRI), in which, an Encoder-Decoder framework is used. Whereas, the complicated encoding process to infer the connections from time series data has limited the scalability and accuracy on larger networks[26]. Further studies promote NRI on several aspects such as the consideration of constraints[24, 51], inferring hidden nodes[52], whereas the problem of scalability and accuracy remains.

However, despite a large amount of experiments on evaluating and comparing various data-driven models have been conducted based on prediction tasks, this is only the first step. According to the three stage ladders of causality, intervention and counterfactual experiments rather than predictions are the golden standards for testing a learned data-driven model as a complete substitution of the original system[29, 53]. That is, the downstream tasks such as the control experiments of both the learned model and the original systems should be tested and compared[54]. However, we found only a few studies have done this kind of tasks[6, 54].

As shown in Figure 1, this paper proposes a unified framework for Automated Interactions and Dynamics Discovery (AIDD). The contributions of this framework includes:

- Large (the number of nodes > 1000) interaction networks can be automatically inferred from time series data with high accuracy ($AUC > 0.9$) by a simple scalable framework;
- Various types of network dynamics (continuous, binary, and discrete) can be learned;
- A new method to verify the data-driven model based on control is proposed;
- The gene regulatory network of yeast *Staphylococcus* network with 100 nodes can be recovered from the time series data generated by GeneNetWeaver platform which simulated real gene dynamics.

Results

Problem Formulation

Without lose generality, suppose the complex system to be considered evolves under discrete time steps. Thus, the dynamics to be reconstructed can be described by a mapping:

$$\mathbf{X}^{t+1} = f(\mathbf{X}^t, A) + \zeta^t, \quad (1)$$

where $\mathbf{X}^t = [X_1^t, X_2^t, \dots, X_N^t] \in \mathbb{R}^{N \times D}$ is the state of the system at time t , N is the number of nodes, D is the dimension of the state space of each single node, A is the adjacency matrix of the interaction network to be inferred, and $\zeta^t \in \mathbb{R}^{N \times D}$ is the noise imposing on nodes. However, Equation 1 can only describe the dynamical processes with explicit mathematical forms and cannot be applied to those defined by rule tables or transitional probabilities, such as cellular automata, boolean dynamics, or Markov chains, etc. Therefore, instead of equation 1, we use a more general form, a Markov chain $\{\mathbf{X}^t\}$, to describe the dynamics:

$$f(\mathbf{X}^{t+1} | \mathbf{X}^t, A) \equiv P(\mathbf{X}^{t+1} | \mathbf{X}^t, A), \quad (2)$$

where, f is the dynamics to be discovered, \mathbf{X}^t is the abbreviation for the event of $\mathbf{X}^t = \mathbf{x}^t$, where $\mathbf{x}^t \in S^N$ is a state value. S is the state space of each single node, which can be either a finite set of discrete values or an infinite set with continuous values. P is a conditional probability. Equation 2 is compatible with Equation 1 and more general than it[55]. It can be even extended non-Markov random processes with finite histories by adding more hidden variables to describe[56].

However, it is difficult to infer the probabilities in equation 2, particularly when N is large. Fortunately, the interactions of complex systems are always localized, which means $P(\mathbf{X}^{t+1} | \mathbf{X}^t, A)$ can be factorized into local transitional probabilities[57]:

$$P(\mathbf{X}^{t+1} | \mathbf{X}^t, A) = \prod_{i=1}^N P(X_i^{t+1} | \mathbf{X}^t \odot A_{.i}), \quad (3)$$

where \odot is the element-wised product, and $A_{.i}$ represents the i^{th} column of matrix A , $\mathbf{X}^t \odot A_{.i}$ is a vector representing the states combination of all neighbor nodes of i . Then

$$f_i(X_i^{t+1} | \mathbf{X}^t \odot A_{.i}) \equiv P(X_i^{t+1} | \mathbf{X}^t \odot A_{.i}) \quad (4)$$

represents the local dynamics of node i , which is also called a causal mechanism in the literature[57].

Therefore, our task becomes to reconstruct the network A and to learn the local dynamics f_i according to the observed time series $\mathbf{x} = (\mathbf{x}^1, \mathbf{x}^2, \dots, \mathbf{x}^T)$ with T time steps on multiple samples.

Model

We build a neural network framework which consists of two modules to solve the reconstruction problem, as shown in the inset panel of Figure 1. The first module is a network generator which can generate a candidate network adjacency matrix $\hat{A}(\Theta)$ with the parameters Θ . The second module then tries to simulate the system dynamics f by using a set of neural networks $\hat{f}_i(\hat{X}_i^{t+1} | \mathbf{x}^t \odot \hat{A}_{.i}(\theta_{.i}), \phi_i)$ for any node i , which are parameterized by $\Phi = (\phi_1, \dots, \phi_N)$ to predict the future state $\hat{\mathbf{X}}^{t+1}, \hat{\mathbf{X}}^{t+2}, \dots$ according to the candidate matrix $\hat{A}(\Theta)$ and the observed state of the previous time step \mathbf{x}^t .

Instead of using the complicated graph network architecture to generate the candidate network as described in [21], we directly sample each element in the adjacency matrix $\hat{A}_{ij} \sim \text{Bernoulli}(\theta_{ij})$, where $\theta_{ij} \in [0, 1]$ represents the probability of that the entry of the i^{th} row and the j^{th} column in \hat{A} is taking the value 1. To make the sampling process differentiable, we use Gumbel-softmax trick[21, 58] to generate the adjacency matrix:

$$\hat{A}_{ij} = \sigma((\log(\theta_{ij}) + \xi_{ij}) / \tau), \quad (5)$$

where $\xi_{ij} \sim \text{Gumbel}(0, 1)$ is a random number following the standard Gumbel distribution, σ is the softmax function, τ is the parameter of temperature to adjust the softness of the sampling process. The random numbers generated by Equation 5 have similar distribution as $\text{Bernoulli}(\theta_{ij})$ especially when τ is large. And the simulated sampling process is differentiable such that the gradients can be passed by. When $\tau \rightarrow \infty$, \hat{A}_{ij} exactly equals 1 with the probability θ_{ij} , or 0 with the probability $1 - \theta_{ij}$.

Compared to other network generation mechanism based on Hadamard product of two V dimensional node feature vectors[8, 21, 25, 46], where $V \ll N$, our method has higher accuracy on inferring links because more parameters ($N \times N$ v.s. $N \times V$) are used.

However, optimizing $N \times N$ parameters does not reduce the implementation performance because the matrix elements are independent each other, which means \hat{A} can be generated column by column separately, where each column represents the possible neighborhood of a single node. In this way, our framework has a large improvement on flexibility and computational efficiency compared to the encoder-decoder frameworks like [21] and it can be applied on very large networks. But the limitations are the networks should be static, and the correlations between elements of \hat{A} are ignored. Further, the introduction of noise ξ_{ij} can push the network generator to jump out of local minimums during the optimization.

According to Equation 3, the dynamics learner can be also decomposed into local modules node by node. Each local dynamics learner can be modelled by a feed-forward or a recurrent neural network $\hat{f}_i(\cdot|\phi_i)$. Both the network structure and the parameters ϕ_i can be either shared by different nodes or not. If they are shared the dynamics learner is a graph network[12, 18, 21]. As shown in Figure 1.

Objective function

Finally, the network inference and dynamics learning problem can be solved by minimizing the following objective function:

$$\begin{aligned} L(\Theta, \Phi) &= \mathbb{E}_{\hat{A} \sim B(\Theta)} \left(-\sum_{t=1}^T \log P(\mathbf{x}^{t+1} | \mathbf{x}^t, \hat{A}, \Phi) \right) + \lambda \sum_{ij} |\theta_{ij}| \\ &\approx -\frac{1}{K} \sum_{k=1}^K \sum_{t=1}^T \sum_{i=1}^N L_i(\mathbf{x}_i^{t+1} | \mathbf{x}^t, \hat{A}_{:,i}^k) + \lambda \sum_{ij} |\theta_{ij}|, \end{aligned} \quad (6)$$

where,

$$L_i(\mathbf{x}_i^{t+1} | \mathbf{x}^t, \hat{A}_{:,i}^k) = \log \hat{f}_i(\mathbf{x}_i^{t+1} | \mathbf{x}^t \odot \hat{A}_{:,i}^k; \phi_i) \quad (7)$$

is the local log-likelihood, and K is the number of samples for matrix \hat{A} under given Θ , and \mathbf{x}_i^t is the observational vector of states of node i at time t . \mathbf{x}^{t+1} is the abbreviation of the event $\hat{\mathbf{X}}^{t+1} = \mathbf{x}^{t+1}$. Thus, the objective function contains two terms, the former is the log-likelihood which can be decomposed into local terms. The later is the structural loss to conform the network to be sparse while avoiding over-fitting[51]. The parameter λ can adjust the relative importance of the structural loss. When we do multiple time predictions, we can replace \mathbf{x}^t in Equation 7 with the prediction in the previous time step, $\hat{\mathbf{X}}^t$ to calculate the loss function.

If the state space S of each node is real, then the local log-likelihood Equation 7 can be taken a mean-absolute-error (MAE) form,

$$L_i(\mathbf{x}_i^{t+1} | \mathbf{x}^t, \hat{A}_{:,i}^k) = \left| \mathbf{x}_i^{t+1} - \hat{f}_i(\mathbf{x}^t \odot \hat{A}_{:,i}^k; \phi_i) \right|, \quad (8)$$

by assuming that $\hat{f}_i(\mathbf{x}_i^{t+1} | \mathbf{x}^t \odot \hat{A}_{:,i}^k)$ is an independent Laplacian distribution for any data point $\frac{1}{(2\nu)} \exp \left[-\frac{1}{\nu} \cdot \left| \mathbf{x}_i^{t+1} - \mu_i(\mathbf{x}^t \odot \hat{A}_{:,i}^k | \phi_i) \right| \right]$, where, the mean value of the Laplacian distribution μ_i is modeled by a neural network $\hat{f}_i(\mathbf{x}^t \odot \hat{A}_{:,i}^k; \phi_i)$, which can be regarded as a new form of the dynamics learner[59]. And $\nu = 1$ in this paper.

Then the network dynamics to fit the observational data can be obtained by optimizing the objective functions Equation 8 node by node[60]. We use stochastic gradient descent algorithm to optimize. More details about training and testing can be referred to the method section and the supplementary information (SI).

Performances and Comparisons

To test our model and compare to others, we generate time series data by a set of network dynamics on a variety of graphs as the ground truths. The continuous, discrete, and binary dynamics are all included. Spring (Spring-mass dynamics)[21], SIR(an inter-city meta-population SIR epidemic model)[61], and Michaelis–Menten kinetics[62, 63] all belong to continuous dynamics. The Coupled logistic Maps Network (CMN)[64, 65] and the voter model[66] are representatives of discrete and binary dynamics, respectively. The graphs to be inferred are either generated by models (ER[67] for Erdos Renyi, WS[4] for Watts-Strogatz, and BA[68] for Barabasi-Albert) or from empirical data including a gene network (for *S.cerevisiae*, Gene), an inter-city traffic network (City) of China, three social networks (Email, Dorm, and Blog), and a road network(Road)[69]. For each model and network, we run the simulation for different times. The generated data is divided into training, validation, and test sets with the ratio of 5:1:1. The validation set is for tuning the hyper-parameters. All the reported results are on the test set.

We compare our model to a series of baseline methods on both network inference and single step forecasting tasks. ARNI and NRI are all the state-of-the-art models on network inference and time series forecasting. The former is based on block-orthogonal regression method, and the latter is based on deep learning and graph network. Another two of the frequently

Table 1. The comparisons of the performances on network inference and dynamics prediction tasks between AIDD and other selected methods (columns) on different dynamics and networks (rows)

Type	Model	Network	ARNI		MI	PC	NRI		LSTM	OURS	
			AUC	MSE	AUC	AUC	MSE/ACC	AUC	MSE/ACC	MSE/ACC	AUC
Con.	Spring	ER-10	0.5853	1.33E-03	0.7500	0.8250	2.60E-08	0.9998*	2.98E-04	2.70E-04*	1.0
		WS-10	0.5125	1.58E-03	0.6875	0.7875	8.40E-08	0.9997*	3.35E-04	3.31E-04*	1.0
		BA-10	0.5169	1.10E-03	0.6422	0.6571	7.00E-10	0.9999*	2.14E-04	2.90E-05*	1.0
		ER-2000	-	-	0.4997	-	-	-	2.25E-03	1.18E-05	0.9886
		WS-2000	-	-	0.5002	-	-	-	5.89E-03	8.51E-06	0.9933
	BA-2000	-	-	0.5010	-	-	-	4.54E-03	2.09E-03	0.9523	
	SIR	SIR-371(D)	0.5424*	8.25E-03	0.5027	0.5119	-	-	2.28E-03*	2.98E-05	0.9156
Menten	Gene-100(D)	1.0	9.71E-03	0.5416	0.6574	-	-	2.29E-03*	4.37E-05	0.9960*	
Dis.	CMN	ER-10	1.0	2.33E-09	0.5745	0.7804	1.40E-05	0.8850	2.60E-04	5.60E-06*	1.0
		WS-10	1.0	2.35E-09	0.6875	0.8375	9.40E-06	0.9331	2.40E-04	2.80E-06*	1.0
		BA-10	1.0	2.40E-09	0.4390	0.7439	1.30E-05	0.6753	9.21E-05	6.90E-06*	1.0
		ER-200	0.8441*	4.17E-02	0.5774	0.7648	-	-	5.91E-05	2.04E-06	0.9987
		WS-200	1.0	2.36E-09	0.6969	0.7506	-	-	1.63E-04	1.95E-06	0.9987*
		BA-200	0.8840*	2.45E-02	0.5533	0.7493	-	-	1.46E-04	2.57E-06	0.9874
		WS-1000	-	-	0.5670	-	-	-	3.54E-05	2.92E-06	0.9795
		BA-1000	-	-	0.5290	-	-	-	3.46E-05	5.48E-05	0.9105
Bin.	Voter	ER-10	-	-	-	0.4552	0.8447*	0.5000	0.5242	0.9647	1.0
		WS-10	-	-	-	0.5250	0.9062*	0.5037	0.6007	0.9463	1.0
		BA-10	-	-	-	0.4607	0.9588*	0.4999	0.6917	0.9866	1.0
		WS-1000	-	-	0.5470*	-	-	-	0.5317	0.6650	0.9996
		BA-1000	-	-	0.5030	-	-	-	0.5208*	0.6758	0.9942
		EMAIL-1133	-	-	0.4999	-	-	-	0.5333*	0.7212	0.9576
		ROAD-1174	-	-	0.5004	-	-	-	0.5455*	0.8942	0.9996
		DORM-217(D)	-	-	0.5219	-	-	-	0.5735*	0.6951	0.9901
		BLOG-1224(D)	-	-	0.4995	-	-	-	0.5295*	0.6793	0.8603

In the network column, we use network - size format. The networks marked with “D” means that they are directed graphs. All networks generated by models share the same edge density value, which is 1% for large networks (size>10), and it is 20% and 3% for small network with size smaller 10, and ER network with size=200, respectively, to avoid isolated nodes. All the results are the averages of repeated experiments for 5 times. Same data volume is shared for different methods in one raw. The data sets for all the machine learning models are separated into train/valid/test sets with 5:1:1. The details of parameters can be referred to SI. The items being marked by “-” indicate that valid results of the model cannot be obtained due to the limitation of the specific method on type of dynamics, and memory or computation time consumption. The best results among all the compared algorithms in the same row are boldfaced, and the second best results are marked “**”.

used statistical metrics, partial correlation and mutual information, are also compared on network inference task. And the classic time series forecasting model, long short term memory (LSTM)[56], is compared on prediction task. In all the experiments, we use a 5-layered feed-forward neural network with 128 hidden units as the dynamics learner(see SI). And the neural network is shared by all nodes. Other parameters are shown in the footnote of Table 1 and SI.

As shown in Table 1, our model outperforms all the methods on large networks for both tasks. Compared with ARNI model, AIDD does not rely on the choice of basis functions, as a result it can be applied on very diverse dynamics. By using neural networks as a universal estimator for dynamics, AIDD avoids the problem of combinatorial explosion of basis functions. This enables AIDD to have competitive performances on space and time complexity ($O(N^2)$ v.s. $O(N^3)$ for ARNI). On very large graphs, ARNI cannot give any result under the limitation of memory and time consumption. In order to compare the performances on time series forecasting, we slightly modified the original algorithm of ARNI such that it can also output one step prediction. Compared to NRI framework, our model has much lighter architecture on network generation. NRI can not output any result under the same limitations of time and space on networks with sizes larger than 30 due to the computational complexity[18].

The model can also output multi-step prediction results by feeding the result of one-step prediction output back to the model. Figure 2 shows the results on selected dynamics.

In general, AIDD can work very well on large sparse networks, and the performances on both tasks decrease as edge density increases as shown in Figure 3(b).

We can improve the accuracy by increasing the amount of data. Figure 3a shows how AUC depends on both network size and data volume to be fed in the model systematically. There is a trade off between network size and data volume under a given accuracy as shown in figure 3 (a). It is interesting to observe that data volume is sensitive to network size only when the number of nodes is in between 300 to 500, and beyond that, a minimum amount of data volume is enough to get an acceptable accuracy (e.g. $AUC = 0.7$), and this is almost not depend on how large is the network.

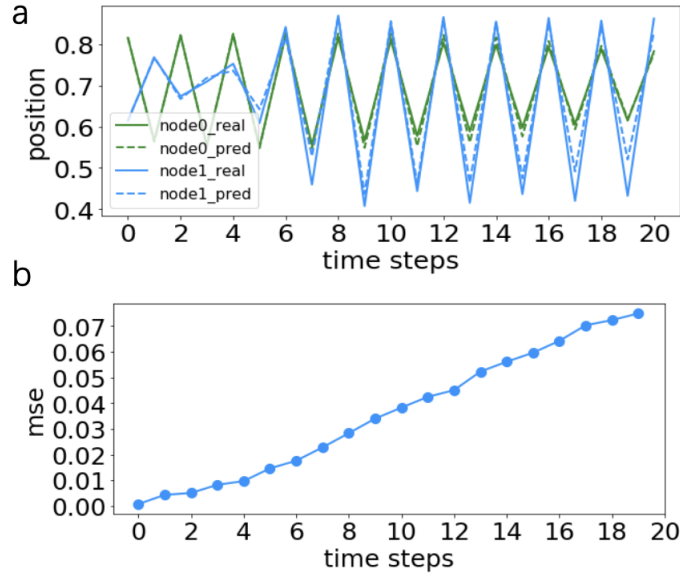


Figure 2. Multi-step prediction results of CMN in a 10-node ER network. In (a), we show the time series data of multi-step predictions and the ground truths for two selected nodes(genes). In (b),we show how mean square error (MSE) increases as time for CMN dynamics. The parameters are same as table 1

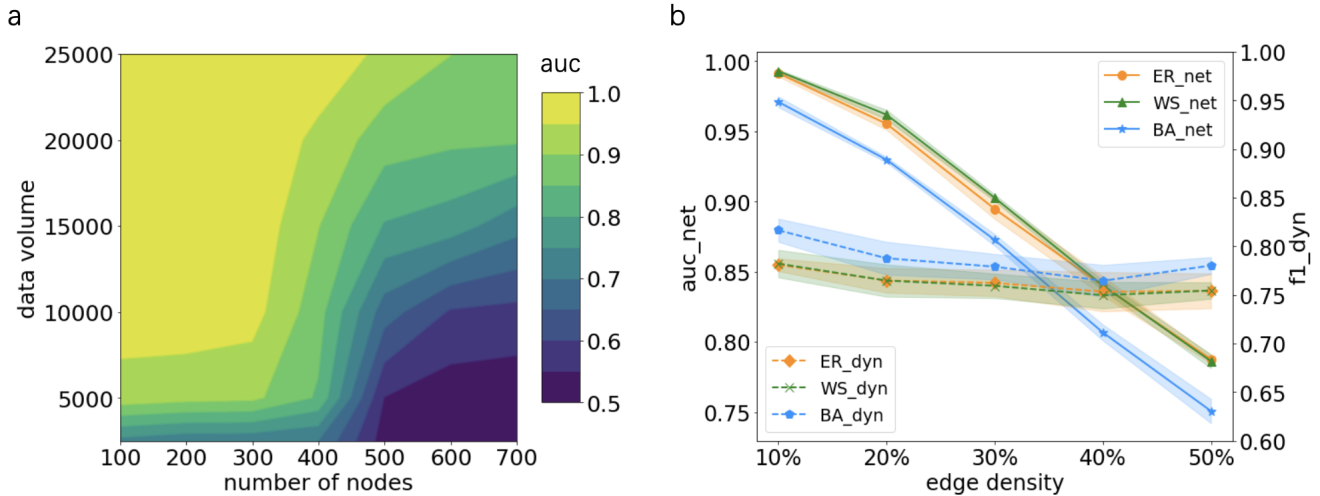


Figure 3. The performances of AIDD under different factors in network inference and dynamics learning. (a) shows how the number of nodes and the volume of data(the number of samples \times the number of time steps which is fixed to 100) jointly influence the network inference accuracy on WS networks under CMN dynamics. And (b) shows how performances decrease with edge density. For the experiments in (b), we fix the number of nodes to 100, and the volume of data to 10 thousand pairs of data, and the sparse matrix parameter λ is set to be 0.

Robustness against noise and hidden nodes

A good data-driven model must be robust against noise and unobservable nodes such that it could be applied on real world. To show the robustness against noise of AIDD, we plot how AUC changes with the magnitude of noise on Michaelis-Menton kinetics which can describe the dynamics on Gene regulatory networks as shown in Figure 4. Our model can recover the network structure with the 0.85 AUC when the magnitude mean of noise is 0.3.

In real applications, we can only obtain the partial information of the entire system due to the limitations of observation. Thus, a certain proportion of nodes are unobservable or hidden. This requires the inference algorithm must be robust on hidden nodes. Thus, we test AIDD on an incomplete network. To generate the incomplete network data as the ground truth, we randomly select a certain percentage of nodes as the hidden nodes (Figure 4(a)), and the time series data of these nodes is

removed. AUC decreases and MSE increases as the fraction of the number of unobserved nodes increases on both Spring and Voter dynamics as shown in figure 4(c), however, the sensitivity depends on different kinds of dynamics. It is found that when the proportion of missing nodes reaches 50%, the inference accuracy is still above 95%, which proves that our model can achieve superior results in the absence of data.

Furthermore, we test the ability of AIDD on revealing unknown network structure of unobservable nodes on CMN and Voter dynamics, but the number of hidden nodes is available. We finish this task by doing the same interaction inference task, and the states for unknown nodes are set by random values. Figure 4(d) shows that the AUCs of the link structures of unknown network on Voter and CMN dynamics. The results reveal that the network inference accuracy is robust on missing nodes. The algorithm can recover the interactions even for the unobservable nodes with more than 80% accuracy.

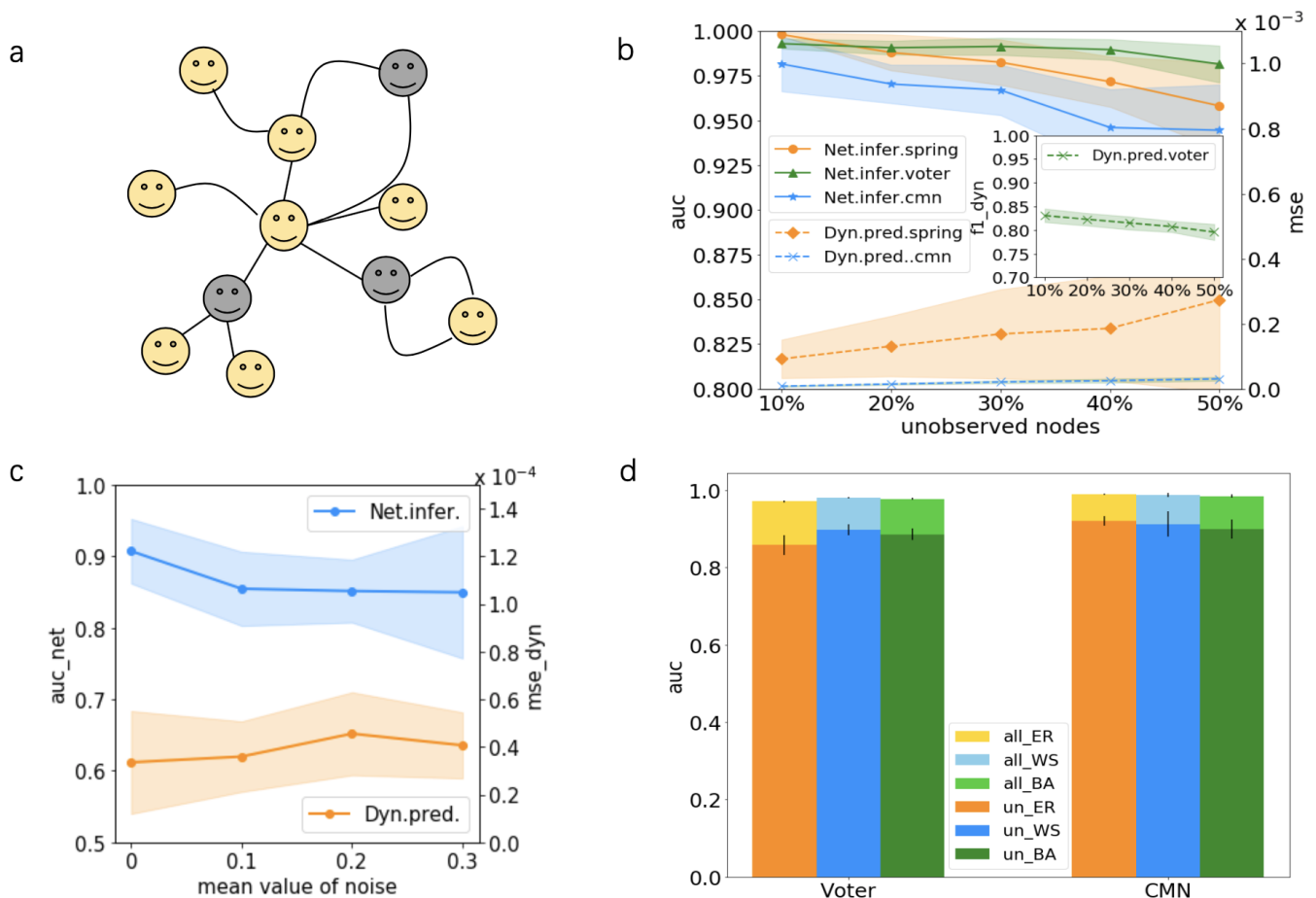


Figure 4. The robustness evaluation of AIDD against noise and missing nodes. (a) shows a ground truth network with missing information on the unobserved nodes (grey nodes). (b) shows how the proportion of the unobserved nodes influences the accuracy of interaction inference on the partial network with observed nodes measured by AUC, and the accuracy of dynamics prediction (inset) measured by the MSE of the observable nodes on Spring, CMN, and Voter dynamics. All the experiments are conducted on an ER network with 100 nodes. (c) shows the dependence of AUC and MSE on the mean of noise added on each node for the Michaelis-Menton kinetics (Gene dynamics) on the yeast *S.cerevisiae* gene network with 100 nodes. (d) shows the ability of AIDD on interaction inferences on the entire networks (the light colored bars) and the unobserved partial networks (the dark color bars). All the experiments are conducted on Spring, CMN, and Voter dynamics with ER, WS, and BA networks, and all networks contain 100 nodes with 10% unobservable nodes selected randomly.

Control

To further verify that if AIDD has learned the ground truth dynamics, and if the learned model can replace the true system, we design control experiments. The reasons why we choose control problem as the test bed for our model include (1) control problem on complex network is very important and it has many engineering backgrounds [6]; (2) control problem is much difficult than predictions. This is true because to control a system means to intervene in it. As a result, we have stood at least on

the second level of the causal ladder[53].

Here, our control problem is to find a control law based on the learned network dynamics such that if the control law is applied on the ground truth model, we can synchronize the whole system by regulating a few nodes. To do this, we divide the nodes in the network into two groups: the driver nodes, who can be manipulated by the controller directly, and the target nodes, whose states cannot be directly controlled, but can be influenced indirectly. The controller is designed via optimizing a set of parameters such that the control objective, that is to synchronize the whole system, is achieved.

The control experiments contain two stages. In the first stage, we find the optimized controller's parameters on the learned network dynamics to achieve the designed objective. And in the second stage, the optimized controller is applied on the ground truth model to evaluate the controller and the learned model. If the same objective can also be achieved on the ground truth model under the regulation of the controller, then the control problem is solved.

Two control experiments are designed. The first one is to synchronize the movement directions of all masses with Spring-mass dynamics on a small size BA network with 10 nodes (see Figure 5 (a)). Three nodes with largest degrees are selected as the driver nodes. And the controller adjusts the forces imposing on the drivers at each time step. The forces are the parameters of the controller to be optimized. The experimental results are shown in Figure 5. The two MSE curves in Figure 5(b) respectively depict the degree of control achieved by the learned model and the ground truth model. They overlap together to show that the learned dynamics can be a good substitute for the real system. Both curves approach 0 within 13 time steps, indicating that the controller has achieved the goal within the given time.

The second control experiment is to ask all the oscillators in a CMN model on a WS model network with 10 nodes (see Figure 5(d)) to take the same value of 0.6, which is the mean of all values one oscillator can take. The controller is a parameterized neural network with five layers, who maps the current state of the system into the control signals. The signals are the forces imposing on the two drivers(with largest degrees) directly. From Figure 6 (e) and (f), the controls are not well be achieved for all nodes since the MSE curves do not converge to zeros. However, the two MSE curves overlap very well which means the surrogate behaves identically as the ground truth model.

Gene regulatory network inference

In order to verify that if our algorithm can be applied on actual scenarios but not only on the toy models, we try to infer the real gene regulatory network from the time series data of mRNA concentrations generated by GeneNetWeaver (GNW)[70], a famous simulator for gene regulatory dynamics.

The networks used by GNW are extracted from known biological interaction networks such as for Escherichia coli or yeast Staphylococcus. On these networks, GNW uses a set of dynamical equations to simulate the transcription and translation process, and has considered many factors closed to real situations. Therefore, GNW is a well known test bed for gene network inference algorithms.

In this experiment, we use different neural networks for each node because more complexity must be handled. The complexity may come from the heterogeneity of node dynamics and the existence of latent variables, noise, and interruptions[70]. We compare our method with partial correlation, Bayesian network inference, and mutual information algorithms in yeast Staphylococcus network with 100 nodes. Our method outperforms others on network inference (Figure 6 (a)) on AUC. It can also predict the dynamics with a relative high accuracy (the average absolute error (MAE) is 0.038, see Figure 6). This manifests that our method can work well on close to real gene regulatory dynamics.

Discussion

In this paper, we propose a unified framework of automatic interaction and dynamics discovery, called AIDD, for large network dynamical systems. We also propose a new standard based on control tasks to evaluate if the true network dynamics can be learned.

The main highlights of AIDD include the scalability, the universality, and the robustness. The high scalability is reflected in that the model can be applied on large network with more than thousands nodes with more than 90% accuracy because the training procedure can be separated on single node. AIDD is a universal framework because it can be applied on different dynamics including continuous, discrete, and binary. AIDD is robust not only on noise in input signal, but also on unobservable nodes. AIDD can recover the entire network even including the part that time series data is missing with more than 90% percent accuracy. AIDD can also work well on data set generated by GeneNetWeaver, which emulates the real environment of gene regulatory network dynamics.

Furthermore, we propose a new method based on controls to test the validity of the learned model. We optimize a controller on the learned model and apply it on both the real system and the model. If they behave similarly, we conclude that the learned model can be the substitute of the real system. Control experiments on Spring and CMN dynamics of small networks have proved that well trained AIDD models can replace the real systems.

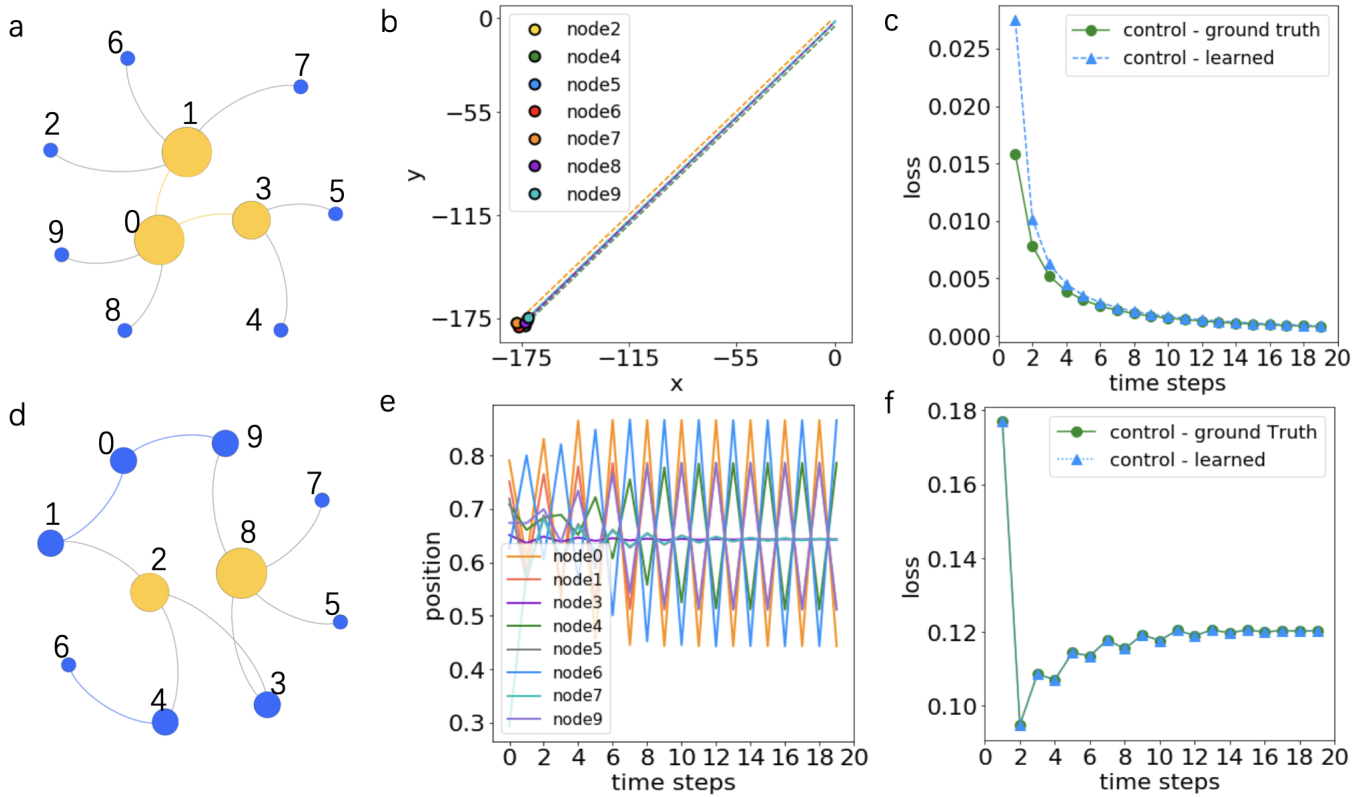


Figure 5. The control experiments on learned models. (a) is the spring network that we studied for the first experiment. Three large nodes are driver nodes, and others are target nodes. The control objective is to ask all masses to have a same movement direction. (b) shows the final movement states of all target nodes under the controls. (c) shows two MSE curves for evaluating goal achievement versus time steps of controls. One curve is on the learned network dynamics, and the other is on the ground truth. (d) is a coupled mapping network that we studied for the second experiment. Two large nodes are selected as driver nodes. The control objective is to ask all oscillators to have the same value of 0.6, which is the mean of the value range for all nodes. (e) shows the oscillations of all target nodes during control. (f) shows two MSE curves for evaluating goal achievement versus time steps of controls. One is for learned model, the other is for the ground truth.

This framework has many potential applications. For example, AIDD can be used to infer missing links according to the dynamics information. AIDD can also be used on time series forecasting. Different from other forecasting models, a clear binary network can be output by AIDD which can provide us more insights about how elements interact and the potential causal links. This increases the explainability of the model.

However, some drawbacks exist in AIDD. First, a large amount of training data, especially the time series in diverse initial conditions, is required to obtain a good model. Nevertheless, it is hard to get different time series under a variety of initial conditions. Although we can split a long time series into segments, and the first values on each segment can be treated as a new initial condition, the diversity of the initial conditions is always not high enough to train an AIDD model with high quality. We may develop new models suitable for small data.

Second, all the dynamics considered in this paper are markovian, but this property is hardly satisfied in real cases. New extensions and experiments on non-markovian dynamics should be conducted. For example, we can use recurrent neural network instead of feed-forward network as the dynamics learner.

Finally, our network generator samples networks according the naive mean field assumption. Although good results have been obtained on network inference, correlations between nodes are ignored. Thus, we can use generative graph models to replace the Bernoulli network generator such that correlations and the inductive bias on structures can be considered.

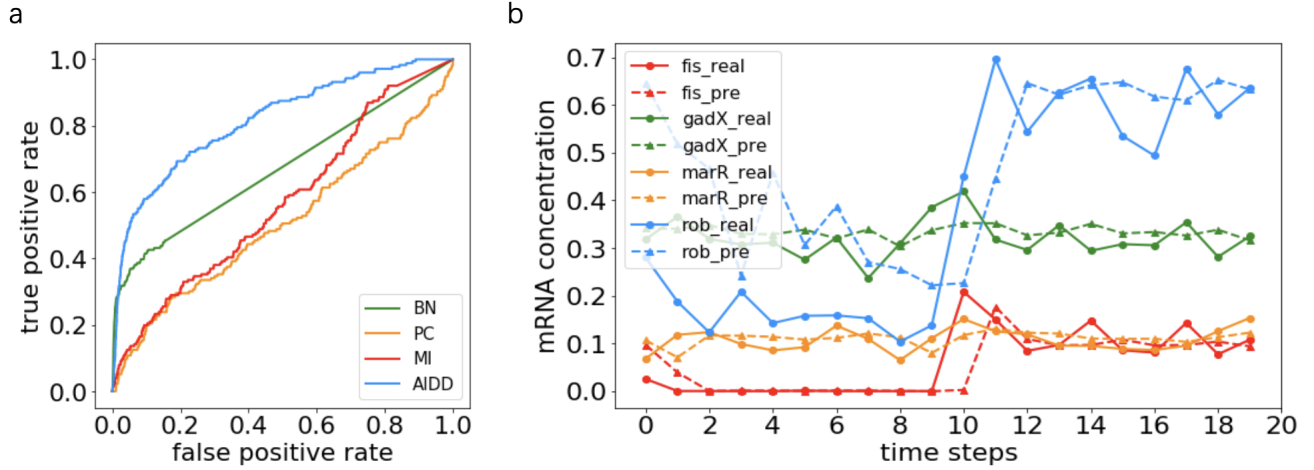


Figure 6. The performances of AIDD on (a) network inference for the gene regulatory network of yeast *Staphylococcus* with 100 nodes, and (b) multi-step time series forecasting. (a) shows the ROC curves of different network inference methods. The comparing methods include Bayesian network (BN), partial correlation (PC), mutual information (MI), and AIDD. (b) shows the comparison between the observed time series of the expression data (real) and the predicted ones on selected genes. In this plot, solid lines represent predictions and the dotted lines represent observed ones.

Methods

Training

We separate the training data by batches, and use stochastic gradient descent algorithm to update the parameters Θ, Φ step by step with different learning rates lr_θ and lr_ϕ , respectively until the epochs of training exceed a threshold. The gradients can be computed directly by automatic differentiation technique on Pytorch platform because all the steps in our framework are differentiable. To improve the efficiency, we sample one adjacency matrix at each epoch and update parameters immediately. The complete algorithm can be referred to SI. We implement the gradient descent algorithm with Adamoptimizer, and all the algorithms are run on RTX 2080Ti(11G).

Network Inference and Time Series Forecasting

After training enough time, the optimized parameters of Θ^* and Φ^* can be obtained. Then we can use network generator to sample the complete adjacency matrices as the inferred networks by setting $\Theta = \Theta^*$ and $\tau \rightarrow \infty$ to obtain absolute 0s or 1s.

Single time step prediction of states for all nodes can be sampled by using the dynamics learner $\hat{\mathbf{x}}^{t+1} \sim P(\hat{\mathbf{X}}^{t+1} | \hat{\mathbf{x}}^t, \hat{A}(\Theta^*), \Phi^*)$, where $\hat{A}(\Theta^*)$ is a sampled adjacency matrix by the optimal parameters. Multiple time step predictions can also be obtained in an independent rollout manner[71], that is to sample the state recursively, $\hat{\mathbf{x}}^{t+1} \sim P(\hat{\mathbf{X}}^{t+1} | \hat{\mathbf{x}}^t, \hat{A}(\Theta^*), \Phi^*)$ for all $t' > 0$. Notice that $\hat{\mathbf{x}}^{t'}$ represents the sample of $\hat{\mathbf{X}}^{t'}$ according to the dynamics learner.

Areas Under the Curve (AUC) and Mean Square Errors (MSE for continuous values) or F1-score (for binary values) are used to evaluate the results of network inference and time series forecasting respectively. More details on training and evaluation can be referred to SI.

References

1. Siegenfeld, A. F. & Bar-Yam, Y. An introduction to complex systems science and its applications. *arXiv preprint arXiv:1912.05088* (2019).
2. Boccaletti, S., Latora, V., Moreno, Y., Chavez, M. & Hwang, D.-U. Complex networks: Structure and dynamics. *Phys. reports* **424**, 175–308 (2006).
3. Bullmore, E. & Sporns, O. Complex brain networks: graph theoretical analysis of structural and functional systems. *Nat. reviews neuroscience* **10**, 186–198 (2009).
4. Watts, D. J. & Strogatz, S. H. Collective dynamics of ‘small-world’ networks. *nature* **393**, 440–442 (1998).
5. Runge, J., Nowack, P., Kretschmer, M., Flaxman, S. & Sejdinovic, D. Detecting and quantifying causal associations in large nonlinear time series datasets. *Sci. Adv.* **5**, eaau4996 (2019).

6. Liu, Y.-Y. & Barabási, A.-L. Control principles of complex systems. *Rev. Mod. Phys.* **88**, 035006 (2016).
7. Wang, W.-X., Lai, Y.-C. & Grebogi, C. Data based identification and prediction of nonlinear and complex dynamical systems. *Phys. Reports* **644**, 1–76 (2016).
8. Ha, S. & Jeong, H. Deep learning reveals hidden interactions in complex systems (2020). [2001.02539](#).
9. Brockwell, P. J., Davis, R. A. & Fienberg, S. E. *Time series: theory and methods: theory and methods* (Springer Science & Business Media, 1991).
10. Wadhvani, R. *et al.* Review on various models for time series forecasting. In *2017 International Conference on Inventive Computing and Informatics (ICICI)*, 405–410 (IEEE, 2017).
11. Benidis, K. *et al.* Neural forecasting: Introduction and literature overview. *arXiv preprint arXiv:2004.10240* (2020).
12. Scarselli, F., Gori, M., Tsoi, A. C., Hagenbuchner, M. & Monfardini, G. The graph neural network model. *IEEE Transactions on Neural Networks* **20**, 61–80 (2008).
13. Battaglia, P. W. *et al.* Relational inductive biases, deep learning, and graph networks. *arXiv preprint arXiv:1806.01261* (2018).
14. Wu, Z. *et al.* A comprehensive survey on graph neural networks. *IEEE Transactions on Neural Networks Learn. Syst.* 1–21, DOI: [10.1109/TNNLS.2020.2978386](#) (2020).
15. Zhou, J. *et al.* Graph neural networks: A review of methods and applications (2019). [1812.08434](#).
16. Zhang, Z., Cui, P. & Zhu, W. Deep learning on graphs: A survey (2020). [1812.04202](#).
17. Yu, B., Yin, H. & Zhu, Z. Spatio-temporal graph convolutional networks: A deep learning framework for traffic forecasting. *arXiv preprint arXiv:1709.04875* (2017).
18. Zang, C., Cui, P., Zhu, W. & Wang, F. Dynamical origins of distribution functions. *Proc. 25th ACM SIGKDD Int. Conf. on Knowl. Discov. & Data Min.* DOI: [10.1145/3292500.3330842](#) (2019).
19. Sanchez-Gonzalez, A. *et al.* Graph networks as learnable physics engines for inference and control. *arXiv preprint arXiv:1806.01242* (2018).
20. Bapst, V. *et al.* Unveiling the predictive power of static structure in glassy systems. *Nat. Phys.* **16**, 448–454 (2020).
21. Kipf, T., Fetaya, E., Wang, K.-C., Welling, M. & Zemel, R. Neural relational inference for interacting systems. *arXiv preprint arXiv:1802.04687* (2018).
22. Zheng, C., Fan, X., Wang, C. & Qi, J. Gman: A graph multi-attention network for traffic prediction. In *Proceedings of the AAAI Conference on Artificial Intelligence*, vol. 34, 1234–1241 (2020).
23. Guo, S., Lin, Y., Feng, N., Song, C. & Wan, H. Attention based spatial-temporal graph convolutional networks for traffic flow forecasting. In *Proceedings of the AAAI Conference on Artificial Intelligence*, vol. 33, 922–929 (2019).
24. Alet, F., Weng, E., Lozano-Pérez, T. & Kaelbling, L. P. Neural relational inference with fast modular meta-learning. *Adv. Neural Inf. Process. Syst.* **32**, 11827–11838 (2019).
25. Wu, N., Green, B., Ben, X. & O’Banion, S. Deep transformer models for time series forecasting: The influenza prevalence case. *arXiv preprint arXiv:2001.08317* (2020).
26. Zhang, Z. *et al.* A general deep learning framework for network reconstruction and dynamics learning. *Appl. Netw. Sci.* **4**, 1–17 (2019).
27. Pareja, A. *et al.* Evolvegen: Evolving graph convolutional networks for dynamic graphs. In *AAAI*, 5363–5370 (2020).
28. Franceschi, L., Niepert, M., Pontil, M. & He, X. Learning discrete structures for graph neural networks (2020). [1903.11960](#).
29. Pearl, J. *Causality* (Cambridge university press, 2009).

30. Tank, A., Covert, I., Foti, N., Shojaie, A. & Fox, E. Neural granger causality for nonlinear time series. *arXiv preprint arXiv:1802.05842* (2018).
31. Löwe, S., Madras, D., Zemel, R. & Welling, M. Amortized causal discovery: Learning to infer causal graphs from time-series data. *arXiv preprint arXiv:2006.10833* (2020).
32. Glymour, C., Zhang, K. & Spirtes, P. Review of causal discovery methods based on graphical models. *Front. genetics* **10**, 524 (2019).
33. Peng, J., Wang, P., Zhou, N. & Zhu, J. Partial correlation estimation by joint sparse regression models. *J. Am. Stat. Assoc.* **104**, 735–746 (2009).
34. Stuart, J. M., Segal, E., Koller, D. & Kim, S. K. A gene-coexpression network for global discovery of conserved genetic modules. *science* **302**, 249–255 (2003).
35. Stetter, O., Battaglia, D., Soriano, J. & Geisel, T. Model-free reconstruction of excitatory neuronal connectivity from calcium imaging signals. *PLoS Comput. Biol* **8**, e1002653 (2012).
36. Nitzan, M., Casadiego, J. & Timme, M. Revealing physical interaction networks from statistics of collective dynamics. *Sci. advances* **3**, e1600396 (2017).
37. Timme, M. & Casadiego, J. Revealing networks from dynamics: an introduction. *J. Phys. A: Math. Theor.* **47**, 343001 (2014).
38. Liu, H., Kim, J. & Shlizerman, E. Functional connectomics from neural dynamics: probabilistic graphical models for neuronal network of caenorhabditis elegans. *Philos. Transactions Royal Soc. B: Biol. Sci.* **373**, 20170377 (2018).
39. Runge, J. Causal network reconstruction from time series: From theoretical assumptions to practical estimation. *Chaos: An Interdiscip. J. Nonlinear Sci.* **28**, 075310 (2018).
40. Casadiego, J., Nitzan, M., Hallerberg, S. & Timme, M. Model-free inference of direct network interactions from nonlinear collective dynamics. *Nat. communications* **8**, 1–10 (2017).
41. Li, L., Xu, D., Peng, H., Kurths, J. & Yang, Y. Reconstruction of complex network based on the noise via QR decomposition and compressed sensing. *Sci. reports* **7**, 1–13 (2017).
42. Granger, C. W. Investigating causal relations by econometric models and cross-spectral methods. *Econom. journal Econom. Soc.* 424–438 (1969).
43. Sugihara, G. *et al.* Detecting causality in complex ecosystems. *science* **338**, 496–500 (2012).
44. Ma, C., Chen, H.-S., Lai, Y.-C. & Zhang, H.-F. Statistical inference approach to structural reconstruction of complex networks from binary time series. *Phys. Rev. E* **97**, 022301 (2018).
45. Rosenblum, M. *et al.* Reconstructing networks of pulse-coupled oscillators from spike trains. *Phys. Rev. E* **96**, 012209 (2017).
46. Veličković, P. *et al.* Graph attention networks. *arXiv preprint arXiv:1710.10903* (2017).
47. Wang, D. *et al.* Learning attribute-structure co-evolutions in dynamic graphs (2020). [2007.13004](https://arxiv.org/abs/2007.13004).
48. Veličković, P. *et al.* Pointer graph networks. *stat* **1050**, 11 (2020).
49. Lachapelle, S., Brouillard, P., Deleu, T. & Lacoste-Julien, S. Gradient-based neural DAG learning (2020). [1906.02226](https://arxiv.org/abs/1906.02226).
50. Wu, Z., Pan, S., Long, G., Jiang, J. & Zhang, C. Graph wavenet for deep spatial-temporal graph modeling (2019). [1906.00121](https://arxiv.org/abs/1906.00121).
51. Li, Y., Meng, C., Shahabi, C. & Liu, Y. Structure-informed graph auto-encoder for relational inference and simulation.
52. Ayed, I., de Bézenac, E., Pajot, A., Brajard, J. & Gallinari, P. Learning dynamical systems from partial observations. *arXiv preprint arXiv:1902.11136* (2019).
53. Pearl, J. & Mackenzie, D. *The book of why: the new science of cause and effect* (Basic Books, 2018).

54. Baggio, G., Bassett, D. S. & Pasqualetti, F. Data-driven control of complex networks (2020). [2003.12189](#).
55. Gardiner, C. W. *et al. Handbook of stochastic methods*, vol. 3 (springer Berlin, 1985).
56. Hochreiter, S. & Schmidhuber, J. Long short-term memory. *Neural computation* **9**, 1735–1780 (1997).
57. Schölkopf, B. Causality for machine learning. *arXiv preprint arXiv:1911.10500* (2019).
58. Jang, E., Gu, S. & Poole, B. Categorical reparameterization with gumbel-softmax. *arXiv preprint arXiv:1611.01144* (2016).
59. Doersch, C. Tutorial on variational autoencoders. *arXiv preprint arXiv:1606.05908* (2016).
60. Lee, J. *et al.* Deep neural networks as gaussian processes. *arXiv preprint arXiv:1711.00165* (2017).
61. Brockmann, D. & Helbing, D. The hidden geometry of complex, network-driven contagion phenomena. *science* **342**, 1337–1342 (2013).
62. Karlebach, G. & Shamir, R. Modelling and analysis of gene regulatory networks. *Nat. Rev. Mol. Cell Biol.* **9**, 770–780 (2008).
63. Barzel, B. & Barabási, A.-L. Network link prediction by global silencing of indirect correlations. *Nat. biotechnology* **31**, 720–725 (2013).
64. Garcia, P., Parravano, A., Cosenza, M., Jiménez, J. & Marcano, A. Coupled map networks as communication schemes. *Phys. Rev. E* **65**, 045201 (2002).
65. Jalan, S., Amritkar, R. & Hu, C.-K. Synchronized clusters in coupled map networks. i. numerical studies. *Phys. Rev. E* **72**, 016211 (2005).
66. Campbell, A., Gurin, G. & Miller, W. E. *The voter decides*. (Row, Peterson, and Co., 1954).
67. Erdős, P. & Rényi, A. On the evolution of random graphs. *Publ. Math. Inst. Hung. Acad. Sci* **5**, 17–60 (1960).
68. Barabási, A.-L. & Albert, R. Emergence of scaling in random networks. *science* **286**, 509–512 (1999).
69. Rossi, R. A. & Ahmed, N. K. The network data repository with interactive graph analytics and visualization. In *AAAI* (2015).
70. Schaffter, T., Marbach, D. & Floreano, D. Genenetweaver: in silico benchmark generation and performance profiling of network inference methods. *Bioinformatics* **27**, 2263–2270 (2011).
71. Tang, C. & Salakhutdinov, R. R. Multiple futures prediction. In *Advances in Neural Information Processing Systems*, 15424–15434 (2019).

Acknowledgements (not compulsory)

We acknowledge the support of the National Natural Science Foundation of China (NSFC) under the grant numbers 61673070.

Author contributions statement

J.Z. conceived the experiments, Y.Z. and Y.G. conducted most of the experiments. Z.Z. and S.W. conducted the experiments of Gene Network, M.Y.C. conducted the experiments of robustness. J.Z., Y.Z., and Y.G. write, and all authors reviewed the manuscript.

Supplementary information

AIDD

The framework consists of two parts: network generator and dynamics learner. The input of the model is the state information of all nodes at time t , and the output of the model is the predicted state information of all nodes at time $t + 1$ and the adjacency matrix.

Due to the assumption that the nodes are separable, our model is trained by nodes. In each epoch of training, the network generator first generates a column of the adjacency matrix that is the neighbor information of the current node, and then inputs the state information of all nodes and a column of A_i of the adjacency matrix generated by the network generator to the dynamic learner. In the experiment, we use a neural network to construct a dynamics learner. The dynamics learner can be divided into four steps: (1) node to edge: aggregating the original information of nodes to form representation vectors of edges; (2) edge to edge: the second step is to encode the information on edges to form new feature vectors of edges; (3) edge to node: aggregate all information on neighbored edges of each node to form a new feature vector of the current node; (4) node to node: finally, we map the hidden representations of nodes to the next step state. The dynamics learner will output the state of the current node in next step. All the mappings are realized by multi-layer feed-forward neural networks. The backward process can be implemented automatically.

In all experiments, we set the hidden layer size of the dynamics learner to 128. The parameter τ in the network generator is set to 1. In our experiment, we set the value of K in the objective function to 1. The reason is that the parameters Θ are sampled at each epoch. During each iteration, the parameters of the network generator and dynamics learner are updated, that is, each epoch is equivalent to one sampling, and the training of multiple epochs is equivalent to Multiple sampling of the network generator under given Θ . The λ in the objective function is the coefficient of the sparse matrix. In the experiment where the number of nodes is less than 1000, λ is set to 0.0001, and when the number of nodes is greater than or equal to 1000, λ is set to 0.001. The data volume in the experiment refers to the number of samples * sampling step size.

Single Step Prediction Algorithm

The algorithm of AIDD is listed in algorithm 1:

Algorithm 1 : Automated Interaction network and Dynamics Discovery, AIDD

```
# parameters
 $N \leftarrow$  Numbers of nodes
 $lr \leftarrow$  Learning Rate
 $s \leftarrow$  Structural Learning Rate
Input:  $X^t$ 
# initialization
Initialize Network Generator parameters  $\alpha$ 
Initialize Dynamics Learner parameters  $\beta$ 
# Training
for each epoch do
  for  $i=1, \dots, N$  do
     $\hat{A}_i \leftarrow$  Gumbel Generator ( $\alpha$ )
     $\hat{X}_i^{t+1} \leftarrow$  Dynamics Learner ( $\hat{A}_i, X^t, \beta$ )
     $loss \leftarrow$  Compute Loss ( $\{\hat{X}_i^{t+1}, X_i^{t+1}\}$ )
     $\delta\beta, \delta\alpha \leftarrow$  BackPropagation
     $\beta \leftarrow \beta - lr * \delta\beta$ 
     $\alpha \leftarrow \alpha - lr * \delta\alpha$ 
  end
   $loss \leftarrow$  Compute Structural Loss ( $\hat{A}$ )
   $\delta\alpha \leftarrow$  BackPropagation
   $\alpha \leftarrow \alpha - lr * \delta\alpha * s$ 
end
Output:  $\hat{A}, \hat{X}^{t+1}$ 
```

Multi-step Prediction Algorithm

AIDD can also be trained and implemented in a multi-step prediction manner, this may improve prediction accuracy. The algorithm of multiple step prediction is listed as algorithm2:

Algorithm 2 : Multi-step Prediction framework

```
# parameters
N ← Numbers of nodes
T ← Steps of prediction
lr ← Learning Rate
s ← Structural Learning Rate
Input:  $X^0$ 
Initialize Network Generator parameters  $\alpha$ 
Initialize Dynamics Learner parameters  $\beta$ 
# Training
for each epoch do
   $\hat{X}^0 \leftarrow X^0$ 
  for  $t=1, \dots, T$  do
    for  $i=1, \dots, N$  do
       $\hat{A}_i \leftarrow \text{Gumbel Generator}(\alpha)$ 
       $\hat{X}_i^t \leftarrow \text{Dynamics Learner}(\hat{A}_i, \hat{X}_i^{t-1}, \beta)$ 
    end
  end
   $loss \leftarrow \text{Compute Loss}(\{\hat{X}^1, \dots, \hat{X}^T\}, \{X^1, \dots, X^T\})$ 
   $\delta\beta, \delta\alpha \leftarrow \text{BackPropagation}$ 
   $\beta \leftarrow \beta - lr * \delta\beta$ 
   $\alpha \leftarrow \alpha - lr * \delta\alpha$ 
   $loss \leftarrow \text{Compute Structural Loss}(\hat{A})$ 
   $\delta\alpha \leftarrow \text{BackPropagation}$ 
   $\alpha \leftarrow \alpha - lr * s * \delta\alpha$ 
end
Output:  $\hat{A}, \{\hat{X}^1, \dots, \hat{X}^T\}$ 
```

Dynamics Model

Spring model

Assuming in a two-dimensional plane, particles are connected to each other by spring. Given the initial position and speed, the masses can move according to spring dynamics. We will use the position and velocity data of each particle generated by the simulation to reconstruct their connection and predict their future position.

We simulate $N \in \{10, 100, 1000, 2000\}$ particles (point masses) in a 2D box with no external forces (besides elastic collisions with the box). We have generated different network structures, which are randomly connected, each pair of particles with a spring. The particles connected by springs interact via forces given by Hooke's law $F_{ij} = -k(r_i - r_j)$ where F_{ij} is the force applied to particle v_i by particle v_j , k is the spring constant and r_i is the 2D location vector of particle v_i . The initial location is sampled from a Gaussian $N(0, 0.5)$, and the initial velocity is a random vector of norm 0.5. Given the initial locations and velocity we can simulate the trajectories by solving Newton's equations of motion PDE. We do this by leapfrog integration using a step size of 0.001 and then subsample each 100 steps for the state of each node on all networks to get our training and testing trajectories, and cut into a training set every two steps.

Coupled Map Network

The coupled map network is characterized by local dynamics operating at each vertex or node of a graph, with these small constituent systems interacting along the edges of the graph. It's a dynamic model describing nonlinear systems, mainly used to study the dynamics of spatiotemporal chaos. The coupled map network is a typical discrete dynamics model. In terms of discrete characteristics, the coupled map network is somewhat similar to a cellular automaton. The state of each cellular automaton depends only on its neighbors. In the coupled map network, the state of each node only depends on its coupled neighbors. The study of the coupled map network model can help us to understand many real systems, such as populations, chemistry, biology, etc. Its definition is as follows:

$$x_i^{t+1} = (1 - \varepsilon)f(x_i^t) + \frac{\varepsilon}{k_i} \sum_{j \in \text{neighbor}(i)} f(x_j^t) \quad (9)$$

$$f(x) = \eta x(1-x) \quad (10)$$

Where ε is the coupling constant and k_i is the degree of node i .

In the experiment, we uniformly sample the initial state from $[0, 1]$, set $\eta = 3.5, \varepsilon = 0.2$, and evolve 100 steps for each node state on all networks.

Voter

In the voter model, the next state of the node is determined by its current state and the state of the node's neighbors. Each node has two states $\{0, 1\}$. Suppose that for a node with degree k , the states of its m neighbors are different from itself at time t , then the node will change its state in the next step with the probability of m/k .

Michaelis–Menten kinetics

Michaelis–Menten kinetics is a non-linear dynamic system model that describes the equations of enzymatic reaction kinetics. They can be derived from ordinary differential equations to describe how the concentrations of related molecular species change. Only some simplified assumptions are needed. Its definition is as follows:

$$\dot{x}_i = -x_i + \frac{1}{n_i} \sum_{j=1}^N J_{ij} \frac{x_j}{1+x_j} + \xi_i \quad (11)$$

Where n_i represents the number of neighbor nodes of the node, J_{ij} represents the directed connection from j to i .

Using the network structure data, the odeint module in python is used to solve the first-order differential equation of the Michaelis-Menten model in order to generate the time series data of the node.

Then the time series data of the node is divided into training set, test set and validation set in a 5:1:1 manner. Input the training set data into our algorithm framework, and finally get a reconstructed adjacency matrix. And as the algorithm has learned the dynamic rules, it can also predict the next state of each node.

SIR

The SIR model is a epidemic model, which is an abstract description of the information dissemination process. The SIR model is the most classic model among infectious disease models, where three states are defined as Susceptible, Infectious, and Recovery. Inter-city traffic can be described by a normalized flux matrix P , then the dynamical model is:

$$s'_n = -as_n i_n + \omega \sum_{m \neq n} P_{nm} (s_m - s_n) \quad (12)$$

$$i'_n = as_n i_n - bi_n + \omega \sum_{m \neq n} P_{nm} (i_m - i_n) \quad (13)$$

$$r'_n = bi_n + \omega \sum_{m \neq n} P_{nm} (r_m - r_n) \quad (14)$$

Where $s_n = S_n/N_n, i_n = I_n/N_n, r_n = R_n/N_n$. a represents the mean infection rate of individual, b represents the mean recovery rate of individual. S_n represents the number of susceptible people in city n , I_n represents the number of infected people in city n , and R_n represents the recovered people in city n , N_n represents the total population of city n , and P is a matrix of intercity traffic based on migration data, where $0 \leq P_{nm} \leq 1$, and P_{nm} quantifies the fraction of the passenger flux with destination m emanating from node n , ω represents the average migration rate.

Networks

Email

Table 2. Network Parameter of Real Network

Network	N	E	$\langle k \rangle$	C
Email	1133	10902	4	0.220
Road	1174	2834	2	0.078
Blog	1224	19025	15	0.210
Dorm	217	2672	24	0.399

This is the email communication network of Rovira i Virgili University in Tarragona, southern Catalonia, Spain. The nodes are users, and each link represents at least one email has been sent. The network is undirected, with 1133 nodes.

Road

This is an international E-road network, which is mainly located in Europe. The network is undirected, with 1174 nodes; The nodes represent cities, and the edge between two nodes represents that they are connected by E-road.

Blog

The network contains homepage hyperlinks between blogs in the context of the 2004 US election. The network is a directed network with 1224 nodes, where nodes represent blogs, and edges represent hyperlinks between two blogs.

Dorm

The network contains friendships among 217 residents living in student dormitories on the Australian National University campus. The network is a directed network with 217 nodes, where nodes represents person, and the edges represents the friendship between two people.

Comparison method

ARNI:(Algorithm for revealing network interactions)

It's a model-independent framework for inferring direct interactions solely from recording the nonlinear collective dynamics generated. First, it systematically decompose each units' dynamics into pairwise, three-point, and higher-order interactions and at the same time treat present influences from one unit to another on the same footing independently of the interaction order. Second, by capturing the structure of the dynamical influences through appropriately chosen basis functions, it posed the reconstruction problem based on nonlinear dynamics as a mathematical regression problem with grouped variables.

For dynamic evaluation, We use MSE as the evaluation indicator, and its calculation method is as follows: $H_{\hat{L}_{i,l}}^{\dagger} H_{L_{i,l}}^n \hat{x}_i$ is the value of \hat{x}_i predicted by the model. Using Euler formula, we have:

$$\hat{X}(t+1) = X(t) + H_{\hat{L}_{i,l}}^{\dagger} H_{L_{i,l}}^n \hat{x}_i \quad (15)$$

We use the predicted state at t+1 and the real state at t+1 to calculate mse.

NRI:(Neural Relational Inference)

It's a variational auto-encoder model that learns to infer interactions while simultaneously learning the dynamics purely from observational data. For the comparison experiment of NRI, we use With the 10-step prediction method, other parameters are the same as those set in the original paper, including the learning rate, the number of hidden layer nodes and so on.

LSTM:(Long Short-Term Memory Network)

It's a well-known recurrent neural network and has been shown to be very suitable for sequence prediction problems. We use LSTM only for node state prediction.

Mutual Information:

This method calculates the mutual information between the probability distributions of the time series of any pairs of nodes. Then a thresholding condition is applied to obtain edges and the roc curve can be plotted. The mutual information method was performed using the Python package netrd.

Partial correlation:

The partial correlation method measures the relationship between two random variables when they are affected by another variable. The method was implemented using the Python package netrd.

Bayesian networks inference:

In a Bayesian network, nodes represent the variables and edges denote the conditional dependencies between random variables. To reconstruct the Bayesian network for genes, we consider each gene as a random variable changing continuously and use the Gaussian Bayesian Networks inference method. A score function named Bayesian Information criterion (BIC) is used to guide the network inference process. This method was performed using the R package bnlearn.

Performance Metrics

In order to evaluate the effectiveness of our model in network inference compared with other models, we use the following indicators to evaluate the effect of network information inference.

AUC:(Area Under Curve)Evaluate the similarity between the probability of network connection learned from the network generator and the real connection matrix. It is defined as the area under the ROC curve and is an index for comprehensive evaluation of accuracy and recall.

MSE:(Mean Squared Error)Measure the expectation of the square of the difference between the true value and the predicted value (estimated value).

ACC:(Accuracy)Evaluate the accuracy of voter dynamics prediction. $ACC = (TP + TN)/(P + N)$

Network Inference under Incomplete Information

In the main text Figure 4d we reported the accuracy on networks with hidden nodes. We complete this task through two steps. First, we run the network inference algorithm1 on the partial observed time series to obtain an adjacency matrix A_1 as shown in 4b, and then we implement a network completion task based on A_1 to complete the links between the unobserved nodes.

The basic idea of the network completion algorithm is to set the initial states of the unobserved nodes as a set of new learnable parameters. Therefore, we can use the similar method listed in Algorithm1 to learn the missing partial network and the initial states of the unobserved nodes. The parameters of dynamics learner can be also fine tuned.

The network completion algorithm is listed in algorithm3:

Control Problem Formulation

Theory

The problem can be formulated as an optimization problem as follows. Suppose the controller optimized on the network and dynamics that we trained is $\hat{C}(X^t, \hat{A}, \hat{f}; \psi_1)$ which can generate a control signal $\hat{U}^t = (U_{d1}^t, U_{d2}^t, \dots, U_{dn}^t, 0, \dots, 0) \in R^{N \times S}$ according to the predicted system state at time step t , and \hat{X}^t for $t = 1, 2, \dots, T_c$ is generated recursively according to the learned network \hat{A} and dynamics \hat{f} . Where, $d1, d2, \dots, dn$ are driver nodes, ψ_1 is the parameter of the controller, and T_c is the maximum time step for the control problem. Similarly, the controller optimized on the real network structure and dynamics is $C(X^t, A, f; \psi_2)$ which can generate a control signal $U^t = (U_{d1}^t, U_{d2}^t, \dots, U_{dn}^t, 0, \dots, 0)$. The following is an example of applying control on the network and dynamics we have learned.

First, the object function can be found by:

$$\min_{\psi_1} J(\tilde{X}_t) = \sum_{t=0}^{T_c} J^t(\tilde{X}_t^{t+1}) \quad (16)$$

Algorithm 3 : Network Completion Algorithm

Input: X_o^t
 $N_o \leftarrow$ Numbers of nodes
 $lr \leftarrow$ Learning Rate
 $s \leftarrow$ Structural Learning Rate
initialization
Initialize Observed Nodes Gumbel Generator parameters α_1
Initialize Observed Nodes Dynamics Learner parameters β_1
Initialize UnObserved Nodes Gumbel Generator parameters α_2
Initialize UnObserved Nodes Dynamics Learner parameters β_2
Initialize Initial States Learner parameters γ
Training Observed Nodes
for each epoch **do**
 for $i=1, \dots, N_o$ **do**
 $\hat{A}_i \leftarrow$ Gumbel Generator (α_1)
 $\hat{X}_i^{t+1} \leftarrow$ Dynamics Learner ($\hat{A}_i, X_o^t, \beta_1$)
 $loss \leftarrow$ Compute Loss ($\{\hat{X}_i^{t+1}, X_i^{t+1}\}$)
 $\delta\beta_1, \delta\alpha_1 \leftarrow$ BackPropagation
 $\beta_1 \leftarrow \beta_1 - lr * \delta\beta_1$
 $\alpha_1 \leftarrow \alpha_1 - lr * \delta\alpha_1$
 end
 $loss \leftarrow$ Compute Structural Loss (\hat{A}_o)
 $\delta\alpha_1 \leftarrow$ BackPropagation
 $\alpha_1 \leftarrow \alpha_1 - lr * \delta\alpha_1 * s$
end
Training UnObserved Nodes
for each epoch **do**
 for $i=1, \dots, N_o$ **do**
 $\hat{X}_m^t \leftarrow$ States Learner (γ)
 $\hat{X}^t \leftarrow (X_o^t \oplus \hat{X}_m^t)$
 $\hat{A}_m \leftarrow$ Gumbel Generator (α_2)
 $\hat{A} \leftarrow (\hat{A}_o \oplus \hat{A}_m)$
 $\hat{X}_i^{t+1} \leftarrow$ Dynamics Learner ($\hat{A}_i, \hat{X}^t, i, \beta_2$)
 $loss \leftarrow$ Compute Loss ($\{\hat{X}_i^{t+1}, X_i^{t+1}\}$)
 $\delta\gamma, \delta\beta_2, \delta\alpha_2 \leftarrow$ BackPropagation
 $\gamma \leftarrow \gamma - lr * \delta\gamma$
 $\beta_2 \leftarrow \beta_2 - lr * \delta\beta_2$
 $\alpha_2 \leftarrow \alpha_2 - lr * \delta\alpha_2$
 end
 $loss \leftarrow$ Compute Structural Loss (\hat{A}_m)
 $\delta\alpha_2 \leftarrow$ BackPropagation
 $\alpha_2 \leftarrow \alpha_2 - lr * \delta\alpha_2 * s$
end
Output: \hat{A}, \hat{X}_o^{t+1}

where, J is a specific problem. We assume that the control signals can be added on driver nodes directly.

Controller Optimization on Learned Model

Our optimization process is as follows:

1. The controller \hat{C} generates the control signal \hat{U}^t .

$$\hat{U}^t = \hat{C}(X^t, \hat{A}, \hat{f}; \psi_1) \quad (17)$$

2. Apply the control signal to the node to get $\hat{U}^t + X^t$, and input it to our learned dynamics learner \hat{f} to get the state after control \hat{X}_t where $\hat{X}_t^{t+1} = (\hat{X}_{t1}^{t+1}, \hat{X}_{t2}^{t+1}, \dots, \hat{X}_{tm}^{t+1})$ m is the number of target node

$$\hat{X}_t^{t+1} = f(\hat{U}^t + X^t) = f(\hat{C}(X^t, \hat{A}, \hat{f}; \psi_1) + X^t) \quad (18)$$

3. Take the objective function as the loss function, carry out gradient back propagation, and constantly update the parameters of the controller ψ_1

4. After the controller is optimized, the optimized controller parameters ψ_1^* of the system are obtained, and the controller is applied to the real network and dynamics to realize the control of specific problems in the real world. As shown in the following formula:

$$\hat{Z}_{ti} = f\{\hat{C}(X^t, A, f, \psi_1^*) + X^t, A_{ti}\} \quad (19)$$

Controller Optimization on Ground Truth Model

At the same time, the baseline of our model is to optimize the controller for specific problems in the real dynamics and network structure, execute the same optimization process above to obtain the control signal U^t and the controller parameters ψ_2^* , and apply the optimized control principle to the real network and dynamics to realize the control of real world. As shown in the following formula:

$$Z_{ti} = f\{C(X^t, A, f, \psi_2^*) + X^t, A_{ti}\} \quad (20)$$

Evaluation and Comparisons

If our method has learned the control principle, then we will get the following formula:

$$\hat{Z}_{ti} \doteq Z_{ti} \quad (21)$$

Algorithm of Controller Optimization

We list the algorithm of controller optimization as algorithm4:

Algorithm 4 : Control Network

```

# parameters
N ← Numbers of all nodes
Tc ← Step of control
lr ← Learning Rate
Input: Xt
# initialization
Initialize Controller Parameters γ
# Training
for each epoch do
  for time=1, ..., Tc do
    # Training Controller
    for i=1, ..., N do
      Ūit ← Controller(Xt, Âi, γ)
      X̂it ← Ūit + Xit
    end
    for j=1, ..., N do
      X̂jt+1 ← Dynamics Learner(X̂it, Âj)
    end
    loss ← Compute Loss({X̂tt+1})
    δγ ← BackPropagation
    γ ← γ - lr * δγ
  end
end
Output: X̂tt+1

```

Table 3. The same parameters for all experiments

hidden_size	lr_net	temp	drop_frac	sample_time	MLP
128	0.04	1	1	1	5 layer

Table 4. Specific experimental parameters

	Experiment	edges_density	network_type	data_num	samples*data_pair	epoch_num	batch_size	lr_dyn	lr_stru
Table1	Spring-10	20%	UnDirected	5000	1*5000	1000	512	0.001	0.00001
	Spring-2000	1%	UnDirected	10000	1*10000	1000	512	0.001	0.001
	SIR-371	2%	Directed	25000	2500*10	1000	2048	0.0033	0.00001
	gene-100	1.95%	Directed	100000	20000*5	1000	4096	0.0033	0.00001
	CMN-10	20%	UnDirected	12000	240*50	1000	2048	0.001	0.00001
	CMN-200	ER:3%WS:1%BA:1%	UnDirected	12000	240*50	1000	2048	0.001	0.0001
	CMN-1000	1%	UnDirected	60000	1200*50	1000	2048	0.001	0.001
	Voter-10	20%	UnDirected	10000	400*25	200	2048	0.001	0.00001
	Voter-1000	1%	UnDirected	50000	2000*25	30	2048	0.001	0.001
	Voter-EMAIL	0.85%	UnDirected	50000	2000*25	30	2048	0.001	0.001
	Voter-ROAD	0.20%	UnDirected	50000	2000*25	30	2048	0.001	0.001
	Voter-BLOG	1.30%	Directed	40000	1600*25	30	2048	0.001	0.001
Voter-DORM	5.67%	Directed	30000	1200*25	200	2048	0.001	0.00001	
Figure 2	CMN	20%	UnDirected	12000	240*50	1000	512	0.001	0.00001
Figure 3	3a	4%	UnDirected	samples*50	samples*50	200	512	0.001	0.0001
	3b	4%	UnDirected	12000	240*50	200	512	0.001	0
Figure 4	4b-Spring	4%	UnDirected	5000	1*5000	1000	512	0.001	0.0001
	4b-CMN	4%	UnDirected	12000	240*50	1000	2048	0.001	0.0001
	4b-Voter	4%	UnDirected	12000	240*50	200	2048	0.001	0.0001
	4d-CMN	4%	UnDirected	12000	240*50	-	1024	-	-
4d-Voter	4%	UnDirected	12000	240*50	-	1024	-	-	
Figure 6	-	1.76%	Directed	10000	-	5000	65536	0.001	0.0001

Application

Spring

For specific control problems such as spring, our objective function is set as follows:

$$J(\tilde{X}_t) = \sum_{t=0}^{T_c} J^t(\tilde{X}_t^{t+1}) = \sum_{t=0}^{T_c} \sum_{i=1}^{m-1} \sum_{j=i+1}^m |v_{ij}^{t+1} - v_{ij}^{t+1}| \quad (22)$$

where $v_{ii}^{t+1} = \frac{v_{ii}^{t+1}}{\|v_{ii}^{t+1}\|_2}$ is the last two dimensions of the X_{ii}^{t+1} , while represents velocity

Coupled Mapping Network

For CMN, our objective function is set as follows:

$$J(\tilde{X}_t) = \sum_{t=0}^{T_c} J^t(\tilde{X}_t^{t+1}) = \sum_{t=0}^{T_c} \sum_{i=1}^n |\tilde{X}_{ii}^{t+1} - P_0| \quad (23)$$

where P_0 is the position when the system is synchronized. The optimization process of the two systems is as discussed in the above process.

Experimental parameters

We list all parameters in the main text as tables.

Specific experimental parameters

Table 5. Other parameters in the experiment for figure-4d

Parameters	Figure 4d - CMN	Figure 4d - Voter
train_epoch	1000	300
com_epoch	1000	300
lr_net	0.004	0.004
lr_dyn	0.001	0.001
lr_net_comp	0.004	0.004
lr_dyn_comp	0.001	0.01
lr_stru	0.0001	0.0001
lr_stru_comp	ER:1e-5,WS:0,BA:0	0
lr_state	0.1	0.05
missing_ratio	0.1	0.1

Table 6. Other parameters in the experiment for figure-5

Experiment	epoch_num	batch_size	lr_con	hidden_size	control_steps
Figure 5b - Spring	1000	512	0.01	128	20
Figure 5b - CMN	1000	512	0.001	128	20